Ionization and equation of state of dense xenon at high pressures and high temperatures

Q. F. Chen,* L. C. Cai, Y. J. Gu, and Y. Gu

Laboratory for Shock Wave and Detonation Physics Research, Institute of Fluid Physics, P.O. Box 919-102, Mianyang, Sichuan, People's Republic of China

(Received 11 August 2008; revised manuscript received 18 October 2008; published 22 January 2009)

The ionization degree and equation of state of dense xenon plasma were calculated by using self-consistent fluid variational theory for temperature of 4–30 kK and density of 0.01–8.5 g/cm^3. The dense fluid xenon will be ionized at high pressures and temperatures. The ionization energy of xenon will be lowered due to the interactions among all particles of Xe, Xe^+, Xe^{2+}, and e. The ionization degree is obtained from nonideal ionization equilibrium, taking into account the correlative contributions to the chemical potential which is determined self-consistently by the free energy function. The composition of xenon has been calculated with given densities and temperatures in the region of partial ionization. The calculated results show a pressure softening regime at the onset of ionization. Comparison is performed with available shock-wave experiments and other theoretical calculations.

DOI: 10.1103/PhysRevE.79.016409 PACS number(s): 52.77.Fv, 62.50.−p, 51.30.+i, 05.70.Ce

I. INTRODUCTION

Noble gases are widely studied in plasma physics because of the simple electric structure such as a closed shell system. Especially, the behavior and equation of state (EOS) of plasma, under the condition of strong heating and compression is of considerable interest from the general physics point of view, it is also of practical interest for astrophysics, the physics of giant planets, and promising applications in power engineering [1]. Various experiments were performed measuring the equation of state and electrical conduction of gas and liquid xenon [2–9]. Different models have also been applied to study the behavior of xenon at ultrahigh pressure. For instance, the augmented-plane-wave (APW) electron band theory method was used to compute the 0-K pressure-volume isotherm [10]. The fluid perturbation theory, employing an interatomic pair potential, was used to calculate the shock-compression curve for comparison with the shock data [10], and the chemical picture was used to determine the ionization composition [11]. Particular attention is being given to the ionization composition of plasma, since this provides a basis for calculating its thermodynamic, transport, and optical properties. Although the chemical picture [11] for fluid xenon at high density took into account the various interactions among atomic and ionic species and electrons, the corrections of lowering of ionization energy caused by the interactions of various particles were not considered in that model. In this paper, a model with chemical reaction based on the chemical equilibrium of ionization is presented, which includes the correction of ionization energy that is determined self-consistently by the free energy function. The theoretical model is described in short, verified by comparing with the available experiments and other calculations, and applied to predict the thermodynamic properties of xenon plasma over a wide range of pressures and temperatures.

II. THEORETICAL MODEL

The model has been described in detail elsewhere [12] but is being expressed here in terms of self-consistent fluid variational theory in order to relate it to our work on dense xenon. The model formulated for xenon at high pressures and temperatures considers that the process of ionization is described shortly in the following. At sufficiently high temperatures and high pressures, supposing that it will produce the first and second ionization processes of xenon, $Xe \rightleftharpoons Xe^+ + e$ and $Xe^+ \rightleftharpoons Xe^{2+} + e$, we have the corresponding equilibrium conditions $\mu_{Xe} = \mu_{Xe^+} + \mu_e$ and $\mu_{Xe^+} = \mu_{Xe^{2+}} + \mu_e$. We neglect above the second ionization stage, consider a plasma consisting of N_e free electrons, N_0 the neutral Xe atoms, N_1 the Xe^+ ions, and N_2 the Xe^{2+} ions in a volume V. The total Helmholtz free energy can be written as

$$F(N_0,N_1,N_2,N_e,V,T) = F^{\mathrm{id}} + F^{\mathrm{conf}} + F^{\mathrm{coul}} + F^{\mathrm{pol}}, \quad (1)$$

where F^{id}, F^{conf}, F^{coul}, and F^{pol} denote contributions to free energy, the ideal, configurational, Coulomb interactions (including electron-electron, ion-ion, and ion-electron), polarization interactions between charged and neutral particles, respectively.

The ideal atomic, ionic, and electronic parts of F^{id} are given by the Maxwell-Boltzmann statistics for the heavy particles and by the Fermi integrals for the electrons,

$$F^{\mathrm{id}} = k_{\mathrm{B}}T\sum_{i=0}^{2} N_i\{[\ln(n_i\Lambda_i^3/Z^{(\mathrm{int})})] - 1\} + N_e k_{\mathrm{B}}T\left(\xi - \frac{2}{3}I_{3/2}(\xi)/I_{1/2}(\xi)\right), \quad (2)$$

where k_{B} is the Boltzmann constant, T is the temperature, n_i is the particle number density, m_i is the mass, and $\Lambda_i = (2\pi\hbar^2/m_i k_{\mathrm{B}}T)^{1/2}$ is the thermal de Broglie wavelength of species i. The internal partition functions

$$Z_i^{(\mathrm{int})} = U_i \exp\left(-\frac{\varepsilon_{i0}}{k_{\mathrm{B}}T}\right),$$

*chenqf01@gmail.com

$$U_i = \sum_{\alpha} g_{i\alpha}\left[\exp\left(-\frac{W_{i\alpha}}{k_B T}\right) - 1 + W_{i,\alpha}/k_B T\right], \tag{3}$$

obey the Brillouin-Plank-Larkin convention, and refer to a common energy scale for all ionization excitation states. ε_{i0} is the bound energy. $g_{i\alpha}$ and $W_{i\alpha}$ are the multiplicity and the energy of excited state α, respectively. Values of these parameters in our model are taken from Moore [13]. In Eq. (2), the electrons are considered as a partially degenerated ideal Fermi gas, $I_n(\xi)$ is the Fermi-Dirac integral

$$I_n(\xi) = \int_0^{\infty} \frac{x^n dx}{e^{x-\xi}+1}, \quad \xi = u_e^{\mathrm{id}}/k_B T. \tag{4}$$

In Eq. (4), u_e^{id} is the ideal part of the chemical potential of the electrons, and ξ can be solved by the following equation:

$$I_{1/2}(\xi) = \frac{\sqrt{\pi}}{2}\frac{N_e \Lambda_e^3}{V}. \tag{5}$$

We treat interactions among neutral species using the fluid perturbation theory of Weeks, Chandler, and Andersen (WCA) [14] and short-range repulsion among ions and atoms using the model of a mixture of hard spheres. In our numerical calculations, atomic and ionic radii for Xe, Xe^+, and Xe^{2+} are taken for the variational parameters determined from the minimization of free energy within self-consistent fluid variational theory (SFVT). The Mansoori formula [15] was adopted to calculate the free energy of multicomponent hard-sphere mixtures of the reference system. A simpler procedure for the ionic sphere radii r_i of species i is based on the assumption that the atom's structure is hydrogenlike [16]. An expansion of the free energy is performed around the contribution arising from the "reference" part, which is almost always approximated by the free energy of a hard-sphere fluid. F^{conf} arises from the free energy of the reference system, the perturbation system can be expressed as

$$F^{\mathrm{conf}} = F^{\mathrm{hs}} + F^{\mathrm{pert}}. \tag{6}$$

The free energy caused by the interactions of atoms can be written as [17]

$$F^{\mathrm{pert}} = \frac{2\pi N_0^2}{V}\int_{d_0}^{\infty} g_{\mathrm{hs}}(r,\eta_0)\Phi(r) r^2 dr, \tag{7}$$

where $\eta_0 = \frac{\pi}{6}\frac{N_0}{V}d_0^3$, $g_{\mathrm{hs}}(r,\eta_0)$ is the hard-sphere radial distribution function. $\Phi(r)$ is the intermolecular potential between xenon atoms, it was taken as the exp-6 form which has been successfully applied to describe the equation of state of many materials over a wide range of densities and temperatures [11].

The Coulomb contributions can be split into four parts as follows:

$$F^{\mathrm{coul}} = F_{ee}^{x} + F_{ee}^{c} + F_{ii}^{c} + F_{ie}^{c}, \tag{8}$$

where superscripts x and c stand for the exchange and correlative contributions, while subscript i stands for ions and e for electrons. The Coulomb interactions are taken as the Padé approximations [18].

The polarization of atoms introduces an additional term in free energy [19]

$$F^{\mathrm{pol}} = \frac{2k_B T}{V} N_0 \sum_i (N_i B_{0,i}), \tag{9}$$

where $B_{0,i}$ is the second Virial coefficient of the polarization potential between atoms and charged species i. It can be expressed as

$$B_{0,i} = 2\pi \int_{\sigma_{\mathrm{Xe}-i}}^{\infty} r^2 (1 - e^{-\beta\phi_{\mathrm{pol}}^i(r)}) dr \quad (i = \mathrm{Xe}^+, \mathrm{Xe}^{2+}, e), \tag{10}$$

where

$$\phi_{\mathrm{pol}}^i(r) = -\frac{Z_i e^2 \alpha_i}{2}\left(\frac{1+r\kappa}{r^2+\sigma_i^2}\right)^2 e^{-2\kappa r} \tag{11}$$

is the polarization potential between xenon and the species i. σ_i and α_i are the hard-core radii of the polarization potential and the polarizability of species i, respectively, and κ is the inverse screen length of the plasma given by [20]

$$\kappa^2 = \frac{3\pi e^2}{k_B T}\frac{N_e}{V}\Theta^{3/2} I_{-1/2}(\mu_e^{\mathrm{id}}/k_B T), \tag{12}$$

where $\Theta = \frac{k_B T}{k_B T_F} = (\frac{4}{3\sqrt{\pi}}\frac{2}{n_e \Lambda_e^3})^{2/3}$, and T_F is the Fermi temperature.

The chemical potentials satisfy the following equations when the system reaches ionization equilibrium:

$$\mu_{i-1} = \mu_i + \mu_e \quad (i = 1,2). \tag{13}$$

Usually, the chemical potentials can be split into ideal parts μ_i^{id} and correlation parts μ_i^c, the above equation can be rewritten as

$$\mu_{i-1}^{\mathrm{id}} + \mu_{i-1}^c = (\mu_i^{\mathrm{id}} + \mu_i^c) + (\mu_e^{\mathrm{id}} + \mu_e^c), \tag{14}$$

where

$$\mu_i^{\mathrm{id}} = \frac{\partial F^{\mathrm{id}}}{\partial N_i}, \quad \mu_e^{\mathrm{id}} = k_B T \xi, \quad \mu_i^c = \frac{\partial F^c}{\partial N_i}, \tag{15}$$

$$F^c = F^{\mathrm{conf}} + F^{\mathrm{coul}} + F^{\mathrm{pol}}. \tag{16}$$

Taking Eqs. (15) and (16) into Eq. (14), the ionization equilibrium equations can be obtained,

$$N_i = K_i N_{i-1} \quad (i = 1,2), \tag{17}$$

where the ionization coefficient $K_i = \frac{U_i}{U_{i-1}}\exp(-\frac{I_i'}{k_B T} - \xi)$, $I_i' = I_i - \Delta I_i$, I_i is the ionization energy, ΔI_i is the correction value, $\Delta I_i = \mu_{i-1}^c - \mu_i^c - \mu_e^c$, and I_i' is defined as the effective ionization energy.

There are five unknown parameters in ionization equilibrium Eqs. (17) and (5), thus two additional equations are needed. Here, two conservation relations of mass and charge can be used

$$N_0 + N_1 + N_2 = N_A, \tag{18}$$

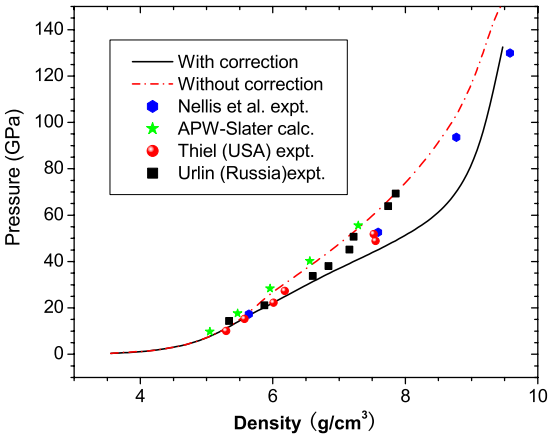

FIG. 1. (Color online) Comparison of liquid xenon Hugoniot.

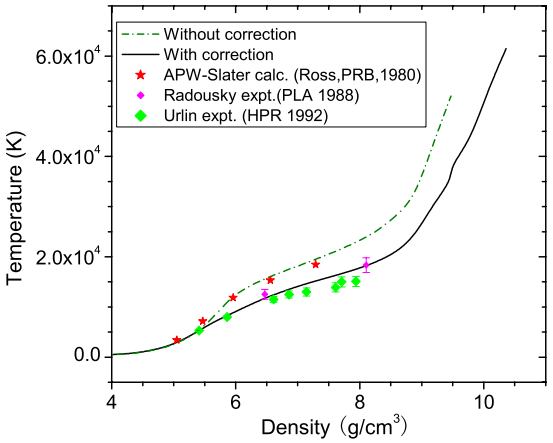

FIG. 2. (Color online) Comparison of the curves for pressure and temperature of liquid xenon along the principal Hugoniot.

$$N_e = N_1 + 2N_2, \tag{19}$$

where N_A is the total number of xenon particles. Then, the particle number and correction ionization can be solved from Eqs. (5) and (17)–(19) by the self-consistent iterative technique.

Once the total free energy has been calculated, the thermodynamic parameters such as pressure, internal energy, and entropy can be obtained from the standard thermodynamic relations. Shock-wave experiments provide us with direct information about a material EOS at high pressure and temperature. When a shock wave passes through the sample, the thermodynamic state of a material, characterized by the internal energy, pressure, and volume, changes from initial (E_0, P_0, V_0) to final values of (E_H, P_H, V_H). The conservation of mass, momentum, and energy yields the Hugoniot condition

$$E_H = E_0 + \frac{1}{2}(P_H + P_0)(V_0 - V_H). \tag{20}$$

Experimental points are deduced from shock velocity measurements so that theoretical models for behavior of materials at high temperatures and pressures can be checked.

III. RESULTS AND DISCUSSION

The equations of state and Hugoniot curve for dense xenon have been calculated using the SFVT as described above. In order to estimate the influence of the lowering of ionization energy caused by the nonideal interactions, we compared the Hugoniot curves derived from the EOS with and without the ionization energy correction. Figure 1 shows our calculation Hugoniot curves of liquid xenon along with experimental data and Ross' calculated results. It is clearly seen that the present calculations with and without the correlative corrections start to deviate at pressure above 20 GPa. The calculations with the correlative corrections show an increase in compressibility related to the calculations without the corrections at the onset of ionization (i.e., $P > 20$ GPa). The Hugoniot curve without considering the ionization energy correction is higher than that with correction. This indicates that the correlative contributions come into play at this pressure above and lead to a measurable softening of Hugoniot. The present results with the correlative corrections are in agreement with the Nellis *et al.* experiments of pressure up to 130 GPa. It is shown that the present model with the correlative corrections can reproduce the experimental shock Hugoniot equation of state. The calculated Hugoniot curve used in the Slater exchange band gap [10] is in agreement with the present calculations without the correlative corrections in the pressure region from 10 to 50 GPa. This indicates that the APW-Slater calculation is not better, including all nonideal interactions.

Shock temperature measurements can provide a test of the theoretical model. It is well known that the ionization equilibrium $Xe \rightleftharpoons Xe^+ + e$ and $Xe^+ \rightleftharpoons Xe^{2+} + e$, etc., reflects the very subtle changes in the electronic and structural properties at high temperature and pressure via the correlative contributions consistent with the equation of state. In order to test the present model, the liquid-xenon shock temperatures versus density have been calculated using the SFVT along the principal Hugoniot. The calculated results along with the APW-Slater [10], Radousky *et al.* [7], and Urlin *et al.* [8] experimental results are shown in Fig. 2. We can see that the present shock temperatures of two calculations with and without the correlative corrections start to deviate at density 5.4 g/cm^3 and the deviation increases gradually with the increase of density. This indicates that the effective ionization energy decreases with the increase of density and temperature. The calculations with the correlative corrections show a decrease in shock temperature related to the calculations without the correlative corrections at the onset of ionization. The calculated shock temperatures with the corrections are in good agreement with the available experiments. The calculation without the corrections is in agreement with the APW-Slater result. This trend is consistent with the calculation of the shock pressure density shown in Fig. 1.

Figure 3 shows the curves of the first and second effective ionization energies ($I_{1\text{eff}}$ and $I_{2\text{eff}}$) of dense xenon as a function of temperature and pressure along the principal Hugoniot. It can be seen that $I_{1\text{eff}}$ and $I_{2\text{eff}}$ will approach the first and second ionization energy (I_{10}=12.12 and I_{20}=21.2 eV)

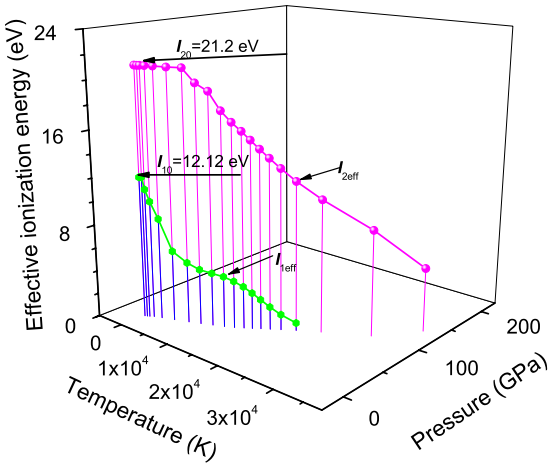

FIG. 3. (Color online) The first and second effective ionization energy of fluid xenon as a function of temperature and pressure along the principal Hugoniot.

of Xe atom at pressure $P \rightarrow 0$ and decrease with the increase of pressure and temperature. The correlative contribution yields a lowering of ionization energy so that pressure ionization becomes operative already in the neutral fluid atoms.

Xenon at high temperatures and pressures is considered the partially ionized plasma. Two ionization stages have been taken into account in our calculations. A comparison of the composition for a density of 1 g/cm^3 is shown in Fig. 4, with and without the correlative corrections. The fraction of onefold and twofold charge ions Xe^+ and Xe^{2+} increase monotonously with increasing temperature in the case of noncorrection at temperature above 12 kK. However, if the corrections are considered, the fraction of onefold charge ions Xe^+ increases up to maximum, then decreases, and the fraction of twofold charge ions Xe^{2+} increases, while the fraction of atoms Xe decreases with the increase of temperature. These systematic trends of the increasing occupation of high ionization stages with increasing temperature are obvious. It is also clearly seen that the effects of the ionization energy correction always lead to higher degrees of ionization as

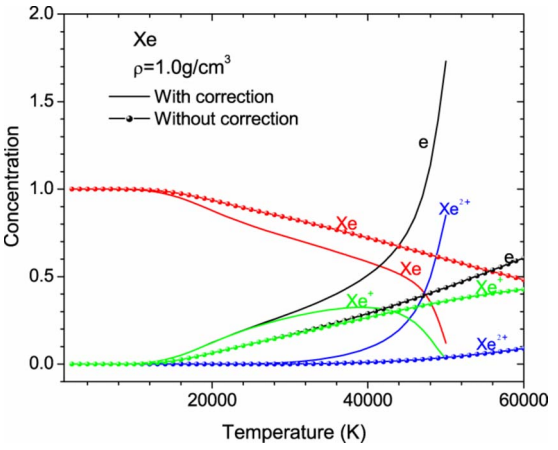

FIG. 4. (Color online) The concentration of ionization composition of xenon plasma as a function of temperature at density $\rho = 1.0$ g/cm^3.

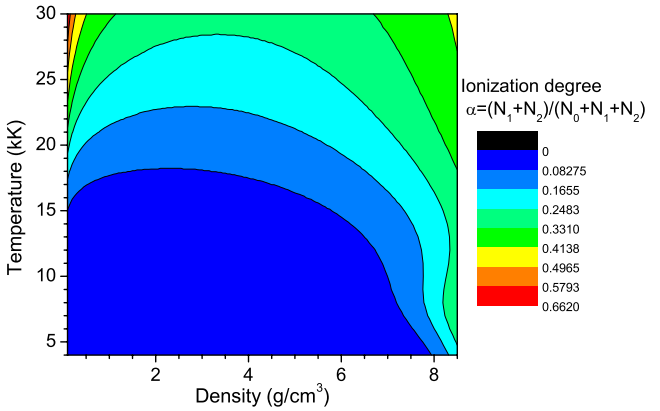

FIG. 5. (Color online) The contour of ionization degree of xenon plasma as a function of temperature and density.

compared with the noncorrection. It verifies the fact that nonideality in a system is always responsible for a decrease of the ionization energy.

Figure 5 shows the contour of ionization degree of fluid xenon as a function of density and temperature in the ranges 0.01–8.5 g cm^{-3} and 4–30 kK. The present model produces pressure and temperature ionization varying continuously as either the density or temperature increases.

Figure 6 shows the predicted contour of the pressure of xenon plasma as a function of density and temperature in the ranges 0.01–8.5 g cm^{-3} and 4–30 kK. It can be seen from Fig. 6 that there is a pressure softening regime in the density ranges 7.5–8.5 g cm^{-3} and the temperature ranges 9–15 kK. This indicates an increase in compressibility at the regime of the onset of ionization. Recently, experimental Hugoniot data for helium have also shown similar results [21]. However, at higher temperature (i.e., $T > 15$ kK) the pressure monotonously increases with the increase of density. This shows that the effect of temperature ionization occurring is dominant.

Physical and chemical pictures provide an alternative description of plasmas. The advantage of the chemical picture is that it is in many cases more appropriate for the description of real plasma. Many chemical picture models have been applied to treat the effect of ionization on the EOS. In these models the atoms, ions, and molecules are treated as

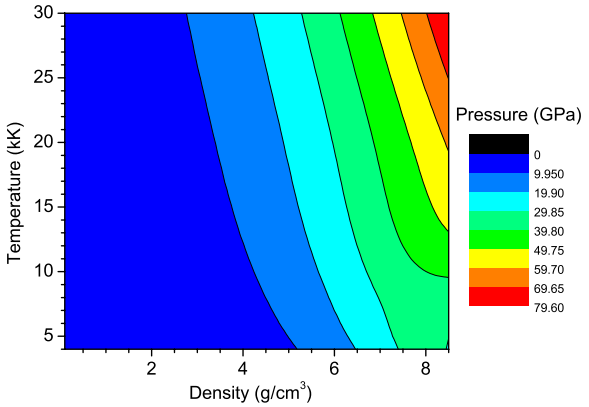

FIG. 6. (Color online) The contour of the pressure of xenon plasma as a function of temperature and density.

separate species. The constituents of the plasma are free electrons, free nuclei, ions, atoms, and molecules. Although the chemical picture for fluid xenon at high density took into account the various interactions among atomic and ionic species and electrons, the corrections of lowering of the ionization energy caused by the interactions of various particles were not considered in that model [11]. However, the treatment of ionization equilibrium in a chemical model has a strong influence on the results for the EOS of dense xenon which is illustrated in Figs. 1, 2, and 4, with and without the correlative corrections. Of special interest for the theoretical description are the correlation contributions of charge particles to the ionization equilibrium as well as between charged and neutral particles. The current chemical model of partial ionization plasmas is proposed. Unlike the ordinary chemical picture it allows one to determine, in a self-consistent manner, both ionization equilibrium and correlative corrections to ionization energy as well. The pressure ionization of hydrogen has been calculated by Saumon and Chabrier [20] using the chemical and ionization equilibrium between the various species. The screened one-component plasma model (SCOP) was applied to treat the Coulomb interactions of the electron-ion system in their model. However, the Coulomb interactions in our model are taken as the Padé approximations which describe the nonideal effects due to exchange and correlation interactions of charged particles and which cover a wide range of densities and temperatures. The Padé approximation formulas are valid at any electron degeneracy, for a very broad region of Coulomb coupling, and are applicable to any chemical mixture [18]. On the other hand, EOS calculations within the more rigorous physical picture, quite successful at relatively low density [22], become prohibitively complicated at high density. First-principles approaches based on path integral Monte Carlo (PIMC) [23] or molecular dynamics (MD) calculations are computationally highly expensive. These methods also suffer from some difficulties. Indeed, the sign or node problem for the PIMC method or the use of effective pair potentials for MD simulations restricts their applicability. In practice, these simulations do not allow the calculation of thermodynamic quantities over a large range of temperatures and densities. In any case, a comparison with our results will be instructive, but, to the best of our knowledge, no PIMC or MD data for xenon in the temperature-density range of interest in this paper has been presented yet.

Although the present calculations are in good agreement with the shocked Hugoniot measurements for dense xenon and helium in the regime of partial ionization, it has some limitations. For example, the multicomponent hard-sphere mixtures of a reference system were employed; the effective interatomic potentials used in the calculations cannot fully reflect the electronic properties and the real many-body effects. The exp-6 potential parameters of xenon only can be used to predict accurately pressure to near 100 GPa [11]. But it is clearly seen from Fig. 1 that the calculated pressures are in good agreement with experiments in the density ranges of $0.01-9.5$ g cm^{-3}. Comparisons with available experimental results demonstrate that the present model calculations can reasonably reproduce the major trends in the basic xenon properties along the principal Hugoniot. However, our predicted equations of state of dense xenon have little difference at density above 9.5 g cm^{-3}. We attribute this difference to the common use of excessively repulsive hard sphere, the exp-6 potentials between the neutral particles, and the polarization potentials between charged and neutral particles as well. At density $\rho > 10$ g cm^{-3}, the solution to ionization equilibrium equations become a formidable task and the computational time consuming by a self-consistent manner, due to the instability of the effective ionization energy caused by the nonideal effects in a system. It leads to the deviations of the calculation model under such high densities, which needs further research.

IV. CONCLUSIONS

The present model considered that the processes of the ionization equilibrium $Xe \rightleftharpoons Xe^+ + e$ and $Xe^+ \rightleftharpoons Xe^{2+} + e$ by self-consistent fluid variational theory can be used to calculate the equation of state of fluid xenon over a wide range of pressure and temperature and reproduce the experimental shock temperatures and Hugoniot equations of state of liquid xenon up to 130 GPa. The calculated results show an increase in compressibility at the onset of ionization. The abundances of the various atomic and ionic components are obtained from the minimization of the free energy. An important feature of the present model is the introduction of the ionization energy correction by fulfilling self-consistently when minimizing free energy under the condition of chemical equilibrium for the first and second ionization reactions. The corrections of ionization energy which are induced by the interactions among all particles of Xe, Xe^+, Xe^{2+}, and e in the self-consistent variational free energy model are taken into account. The influence on the equation of state is analyzed via considering both with and without the ionization energy correction. The present model represents a significant effect to describe the interaction properties in a dense mixture of atoms, electrons, and ions. The results for the degree of ionization can provide a basis for calculating the electrical conductivity, transport, and optical properties. The present model can be extended to the calculated EOS of other chemical elements, such as argon, krypton, and oxygen, etc. Some approximations, such as the hard-sphere model and Padé approximations are taken into account in our model, which may result in a bit uncertainty in the calculation. Highly ionized xenon will occur at ultrahigh pressures and temperatures, the contributions to the overlapping of the electronic cloud and the density dependence of atomic partition function should be taken into account for the theoretical description. This will be our aim in further work.

ACKNOWLEDGMENTS

This work was supported by the National Natural Science Foundation of China (Grant No. 10674120), by the Science and Technology Development Foundation of China Academy of Engineering Physics (Grant No. 2007A01002), and by the Foundation of Laboratory for Shock Wave and Detonation Physics Research, China Academy of Engineering Physics (Grant No. 9140C67120206ZS7502).

[1] R. Paul Drake, *High Energy Density Physics:Fundamental Inertial Fusion, and Experimental Astrophysics* (Springer, Berlin, 2006), p. 5.
[2] W. J. Nellis, M. van Thiel, and A. C. Mitchell, Phys. Rev. Lett. **48**, 816 (1982).
[3] V. D. Urlin, M. A. Mochalov, and O. L. Mikhailova, Mat. Model. **3**, 42 (1991) (in Russian).
[4] V. E. Fortov, A. A. Leontev, A. N. Dremin, and V. K. Gryaznov, Zh. Eksp. Teor. Fiz. **71**, 225 (1976) (in Russian).
[5] V. K. Gryaznov, M. V. Zhernokletov, V. N. Zubarev, I. L. Iosilevsky, and V. E. Fortov, Zh. Eksp. Teor. Fiz. **78**, 573 (1980) (in Russian).
[6] S. Kuhlbrodt, R. Redmer, H. Reinholz, G. Ropke, B. Holst, V. B. Mintsev, V. K. Grayaznov, N. S. Shilkin, and V. E. Fortov, Contrib. Plasma Phys. **45**, 61 (2005).
[7] H. B. Radousky and M. Ross, Phys. Lett. A **129**, 43 (1988).
[8] V. D. Urlin, M. A. Mochalov, and O. L. Mikhailova, High Press. Res. **8**, 595 (1991).
[9] V. E. Fortov, V. Ya. Ternovoi, M. V. Zhernokletov, M. A. Mochalov, A. L. Milkhailov, A. S. Filimonov, A. A. Pyalling, V. B. Mintsev, V. K. Gryaznov, and I. L. Iosilevskii, J. Exp. Theor. Phys. **97**, 259 (2003).
[10] M. Ross and A. K. McMahan, Phys. Rev. B **21**, 1658 (1980).
[11] V. Schwarz, H. Juranek, and R. Redmer, Phys. Chem. Chem. Phys. **7**, 1990 (2005).
[12] Q. F. Chen, Y. Zhang, L. C. Cai, Y. J. Gu, and F. Q. Jing, Phys. Plasmas **14**, 012703 (2007).
[13] C. E. Moore, Natl. Stand. Ref. Data Ser. (U.S., Natl. Bur. Stand.) **35**, 113 (1971).
[14] F. Perrot and M. W. C. Dharma-Wardana, Phys. Rev. A **30**, 2619 (1984).
[15] G. A. Mansoori, N. F. Carnahan, K. E. Starling, and T. W. Leland, J. Chem. Phys. **54**, 1523 (1971).
[16] V. K. Gryaznov, V. E. Fortov, M. V. Zhernokletov, M. A. Mochalov, G. V. Simakov, R. F. Trunin, L. I. Trusov, and I. L. Iosilevskii, J. Exp. Theor. Phys. **87**, 678 (1998).
[17] M. Ross, J. Chem. Phys. **71**, 1567 (1979).
[18] W. Stolzmann and T. Blocker, Astron. Astrophys. **314**, 1024 (1996); **361**, 1152 (2000).
[19] H. Reinholz, R. Redmer, and S. Nagel, Phys. Rev. E **52**, 5368 (1995).
[20] D. Saumon and G. Chabrier, Phys. Rev. A **46**, 2084 (1992).
[21] J. Eggert, S. Brygoo, P. Loubeyre, R. S. McWilliams, P. M. Celliers, D. G. Hicks, T. R. Boehly, R. Jeanloz, and G. W. Collins, Phys. Rev. Lett. **100**, 124503 (2008).
[22] F. J. Rogers, F. J. Swenson, and C. A. Iglesias, Astrophys. J. **456**, 902 (1996).
[23] V. Bezkrovniy, V. S. Filinov, D. Kremp, M. Bonitz, M. Schlanges, W. D. Kraeft, P. R. Levashov, and V. E. Fortov, Phys. Rev. E **70**, 057401 (2004).